J Electr Eng Technol Vol. 8, No. 3: 581-587, 2013
http://dx.doi.org/10.5370/JEET.2013.8.3.581

ISSN(Print) 1975-0102
ISSN(Online) 2093-7423

Optimal Design of Low-Speed Secondary-Sheet Single-Sided Linear Induction Motor

Abbas Shiri† and Abbas Shoulaie*

Abstract – Among different linear motors, single-sided linear induction motors have been widely used in industry due to their simplicity and low construction cost. However, these types of motors suffer from low efficiency and power factor. In this paper, an effective procedure is proposed to design single-sided linear induction motors. The designed motor is simulated in MATLAB software in order to investigate the effect of design parameters on the performance of the machine. Regarding the obtained results, the Genetic Algorithm is employed to optimize the design considering product of efficiency and power factor as objective function. The results show significant improvement of the performance. Finally, experimental results and 2D finite element method is used to validate the model parameters and the optimization results.

Keywords: Efficiency, Genetic algorithm, Magnetic air-gap, Optimization, Power factor, Thrust

1. Introduction

Recently, secondary-sheet single-sided linear induction motors (SLIMs) are widely used in industry especially in transportation systems due to their compatible structure and flexible choice of railroad [1-3]. Different methods such as equivalent circuit model, electromagnetic field analysis and finite-element method have been proposed for designing linear induction motors (LIMs) [4-7]. Despite different merits, SLIMs have some disadvantages such as low efficiency and power factor. Hence, proper performance of these motors requires optimization of their design, considering different outputs as objective functions. In literature, different objective functions have been presented for optimization of the LIM. In reference [8] the primary weight has been considered as objective function. In other work, the thrust and power to weight ratio are maximized [9]. In [10] and [11] optimum winding design of LIM have been presented. In other researches, optimal design of the LIM for having the maximum thrust and the power factor has been done [12, 13]. In the latter works, the primary current density, the primary width to pole pitch ratio and the secondary aluminum sheet thickness have been selected as design independent variables. In [14] imperialist competitive algorithm is used to design SLIM. In this work, the design is not validated by FEM or experiment. In addition, it seems that the flux density in different parts of the motor has not been limited. According to literature, there is not a systematic method for designing SLIMs. In this paper, a computer-aided systematic and simple design algorithm is proposed for SLIM. In the proposed algorithm, different geometries of the machine are calculated using analytical equations. Then, the low speed SLIM design is optimized based on the equivalent circuit model and using Genetic algorithm. Experimental tests are done on a constructed laboratory prototype to evaluate the precision of the model parameters used in design. To confirm the validity of the optimization, finite element method is employed and the results are compared.

† Corresponding Author: Dept. of Electrical Engineering, Iran University of Science and Technology, Iran. (abbas_shiri@iust.ac.ir)
* Dept. of Electrical Engineering, Iran University of Science and Technology, Iran. (shoulaie@iust.ac.ir)
Received: January 7, 2012; Accepted: January 14, 2013

2. Calculation of Slot Dimensions

The structure of the single-sided linear induction motor as well as its teeth and slot dimensions are shown in Fig. 1. In this figure g is mechanical clearance. Regarding the magnetic permeability of the aluminum, in calculations, the mechanical clearance is replaced with magnetic air gap. The magnetic air gap is defined as:

$$g_m = g + d \tag{1}$$

where d is the thickness of the secondary sheet. Considering the concept of current sheet and slotted structure of the primary, the magnetic air-gap will increase to effective air-gap which is given by [15]:

$$g_e = k_c g_m \tag{2}$$

In the above equation, k_c is Carter's coefficient which is given by:

$$k_c = \tau_s / (\tau_s - \gamma g_m) \tag{3}$$

where τ_s is the slot pitch and is equal to:

$$\tau_s = \tau / mq \tag{4}$$

According to [16] γ in Eq. (3) is given by:

$$\gamma = \frac{(w_s / g_m)^2}{5 + (w_s / g_m)} \tag{5}$$

where w_s is the slot width which is calculated by:

$$w_s = \tau_s - w_t \tag{6}$$

In Eq. (6) w_t is the tooth width. The primary slot depth can be simply calculated by the following equation (see Fig. 1):

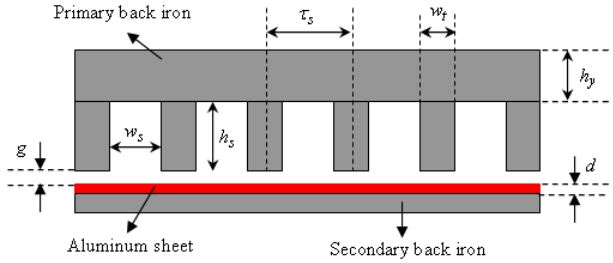

Fig. 1. Single-sided linear induction motor

$$h_s = A_s / w_s \tag{7}$$

where A_s is the cross-sectional area of the primary slot which is given by:

$$A_s = n_c A_w / F_{fill} \tag{8}$$

In the above equation, A_w is the cross-sectional area of the conductor, F_{fill} is fill factor of the slot and n_c is the number of conductors per slot which is equal to:

$$n_c = N / pq \tag{9}$$

where N is the number of turns per phase. Number of turns per coil, n_{coil} can be calculated using n_c. For single-layer winding $n_c = n_{coil}$, and for double-layer winding $n_c = 2n_{coil}$.

3. Equivalent Circuit Parameters

For the design of SLIM with negligible end effect, a simple magnetic equivalent circuit model is used. The per-phase equivalent circuit model of SLIM is shown in Fig. 2. In this figure different parameters are given as follows [16]:

$$R_1 = 2(W_s + l_{ec})N / (\sigma_w A_w) \tag{10}$$

$$X_1 = \{2\mu_0\omega_1[(\lambda_s(1+\frac{3}{2p}) + \lambda_d)\frac{W_s}{q} + \lambda_e l_{ce}]N^2\} / p \tag{11}$$

$$X_m = 12\mu_0 f_1 W_{se} k_w{}^2 N^2 \tau / (\pi p g_e) \tag{12}$$

$$R_2' = 6W_s k_w{}^2 N^2 / (p\tau\sigma_s d) \tag{13}$$

In the above equations σ_w is the conductivity of the conductor used in the primary winding, l_{ec} is the end connection length (usually it is supposed to be $l_{ec} = 1.2\tau$), W_s the primary width, N the number of turns per-phase of the primary winding, A_w the cross-sectional area of the conductor, μ_0 the permeability of air, p the number of pole pairs, q the number of the slots per pole per phase, f_1 input frequency and λ_s, λ_e and λ_d are the permeances of slot, end connection and differential, respectively. Also, k_w is the winding factor, τ the pole pitch, g_e the effective air-gap and σ_s is the conductivity of the secondary sheet. In addition, W_{se} is the effective equivalent primary width which is calculated by the following equation:

$$W_{se} = W_s + g_m \tag{14}$$

In secondary sheet linear induction motors, the secondary reactance can be neglected [6]. Also, due to law value of flux density in the air-gap, core loss is negligible.

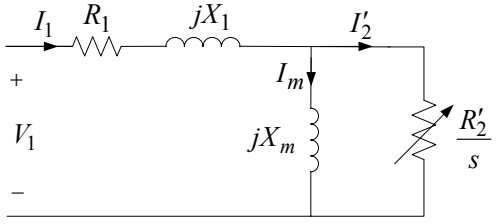

Fig. 2. Equivalent circuit of sheet secondary SLIM

Considering Fig. 2 and doing some mathematical calculations, the following equations for efficiency, power factor and thrust are derived [16]:

$$\eta = \frac{F_x V_r}{3V_1 I_1 \cos\phi} \tag{15}$$

$$\cos\phi = [F_x 2\tau f_1 + 3I_1{}^2 R_1] / (3I_1 V_1) \tag{16}$$

$$F_x = \frac{3I_1{}^2 R_2'}{s2\tau f_1[(\frac{1}{sG})^2 + 1]} \tag{17}$$

where V_r is the motor speed, s is the slip and G is the goodness factor which is calculated as follows [16]:

$$G = 2\mu_0 f_1 \tau^2 \sigma_s d / (\pi g_e) \tag{18}$$

Air-gap flux density is given by [16]:

$$B_g = \mu_0 J_m \tau / [\pi g_e \sqrt{1+(s.G)^2}] \quad (19)$$

In the above equation, J_m is amplitude of equivalent current sheet which is calculated as follows [16]:

$$J_m = 3\sqrt{2} k_w N I_1 / (\pi \tau) \quad (20)$$

Using Eq. (19), the teeth flux density is obtained by:

$$B_t = B_g \tau_s / w_t \quad (21)$$

4. Experimental Validation of the Equivalent Circuit Parameters

In this paper, the SLIM is designed using the equivalent circuit model. So, the effectiveness of the design mainly depends on the validity of the model parameters. In this section, calculation results of the SLIM parameters are compared with those obtained by experimental tests. In [17], the standard test procedure for obtaining rotating induction motor (RIM) parameters is described. Similar to the RIMs, three tests are required to determine the parameters of the SLIM: DC test, primary locked test and no-load test. In case of RIM, at no-load test, due to the fact that the slip of the motor approximately approaches to zero, the rotor impedance can be neglected in comparison with the magnetizing branch impedance. Also, in rotor-locked test, due to the fact that the rotor impedance is much smaller than the magnetizing branch impedance, the latter can be neglected in calculations. However, in case of the SLIM those simplifying assumptions are not applicable. Because, in SLIMs, due to high value of the air-gap and special construction of the secondary, the magnetizing impedance is low and the secondary resistance is high in comparison with RIMs. Also, because of the friction between the primary and the rail at no-load, the slip of the motor is not very small. So, along with mentioned test results, a set of non-linear equations should be solved to accurately determine the SLIM parameters.

The primary locked and no-load tests are done on a constructed prototype in laboratory. The specification of the constructed SLIM is presented in Table 1. Fig. 3 shows the motor input currents in no-load test. The results of the primary locked and no-load tests are given in Table 2. By using experimental results and solving non-linear equations, the motor parameters are derived and compared with calculation results in Table 3. It is seen in this table that the error of the primary parameters are quiet negligible. Also, the error of the magnetizing inductance and the secondary resistance are acceptable. The largest error is related to the magnetizing inductance which is -4.27%.

Table 1. The specification of the constructed SLIM

Phase input voltage, v	220	Slot depth, mm	25
Supply frequency, Hz	50	Aluminum thickness, mm	4
Pole pairs	2	Secondary back-iron width, mm	10
Slots/pole/ phase	1	Mechanical clearance, mm	3.5
Primary width, mm	45	Number of turns/phase	1100
Secondary width, mm	170	Motor length, mm	204
Tooth width, mm	6	Synchronous speed, m/s	4.95
Slot width, mm	10	Rail length, m	81

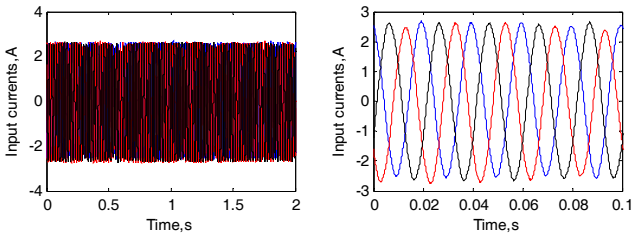

Fig. 3. The SLIM input currents in no-load test

Table 2. Primary locked and no-load tests results

Primary locked test	Input phase voltage, V	216
	Input current, A	1.89
	Input power, W	618.5
No load test	Input phase voltage, V	220
	Input current, A	1.86
	Input power, W	458.2
	Motor speed, m/s	4.28

Table 3. The SLIM parameters: comparison of calculation results with experimental results

Parameter	Calculation	Experiment	Error, %
Primary resistance, Ω	37.46	37.27	-0.51
Primary leakage inductance, mH	221.4	219.6	-0.82
Magnetizing inductance, mH	139.1	133.4	-4.27
Secondary resistance, Ω	32.29	33.59	+3.87

4. Design Procedure

Equation (15) is basically used to initialize the design process. In this equation, the primary current can be estimated using the motor desired parameters:

$$I_1 = F_{xd} V_r / (3 V_1 \eta \cos\phi) \quad (22)$$

Where F_{xd} is the desired thrust should be produced by the designed motor. Now having desired thrust, motor speed, input voltage and proper value for $\eta \cos\phi$, the required input current can be calculated. In this paper, the design procedure is in such a way that the motor can finally produce the desired thrust. Thus to began with, the number of turns per coil (n_{coil}) is set to 1 and increased by 1 until the thrust requirements in the design are met. In each step, the calculated thrust is compared with the desired value. If the error is acceptable the process is stopped. The flow chart of the design is shown in Fig. 3. In this flow chart the

value of $\eta\cos\phi$ is initially chosen arbitrarily in [0 1] span. Then, in the next stage of the algorithm, its value is compared with the calculated value $[\eta\cos\phi]_{cal}$. If the two values are approximately equal, the algorithm is proceeded otherwise the value of $\eta\cos\phi$ replaced by their mean value and the calculation is repeated. Also, in this design in order to prevent the saturation of the iron, the flux density in teeth is compared with a predefined maximum flux density. If the teeth flux density is higher than its maximum value, the arrangement of the turns in slot is changed.

Table 4 shows the specification of the designed motor. In this design the obtained value of the number of turns per coil, n_{coil} is 87 (single-layer winding is used). With this number of turns, the thrust of the motor is approximately equal to its desired value. In addition, the efficiency and power factor are obtained 46.15% and 0.1921, respectively; and the primary winding and iron weight are 3.73 and 3.41 kg, respectively.

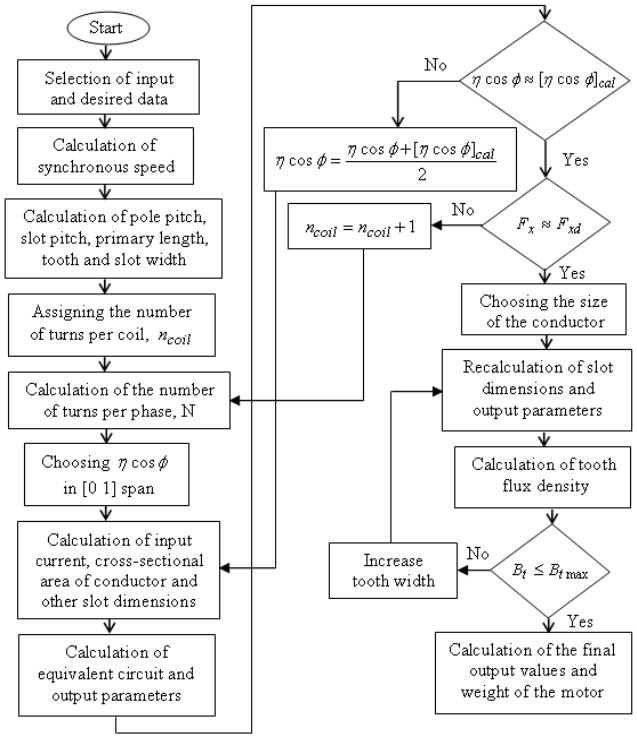

Fig. 3. Flow chart of the SLIM design

Table 4. The specification of the designed motor

Input phase voltage, v	220
Supply frequency, Hz	50
Number of pole pairs, (p)	2
Rated slip	0.3
Number of slots/pole/phase(q)	1
Primary width, mm	150
Thickness of the secondary sheet, mm	3
Primary current density, A/mm^2	5
Desired thrust, N	128
Rated speed, m/s	2.5
Mechanical clearance, mm	1

5. Simulation Results and Motor Performance Analysis

In this section, to investigate the effect of the design parameters such as the mechanical clearance, the secondary sheet thickness, the primary width, etc. on motor performance, the designed linear induction motor is simulated using MATLAB software. For optimization problem, the reaction of the motor to independent design parameters should be considered.

Fig. 4 illustrates the effect of changing the secondary sheet (Aluminum) thickness on the motor outputs (other design parameters are kept constant, see Table 4). As it is seen in the figure, by increasing the aluminum thickness, on the one hand, the goodness factor of the motor, which is one of the important factors in machine design, increases; on the other hand, the thrust and the power factor increase until they reach a maximum value, then decrease, while the motor efficiency increases initially and then noticeably decreases. As a result, to select a proper value for aluminum thickness, there should be a compromise between different outputs such as efficiency, thrust and power factor. The variation of the outputs with changing the mechanical

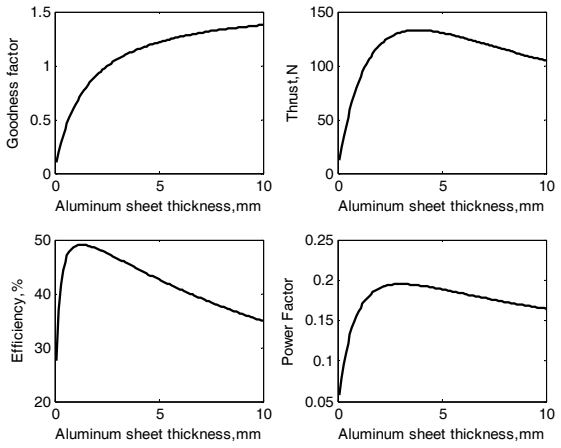

Fig. 4. The motor outputs versus the aluminum thickness

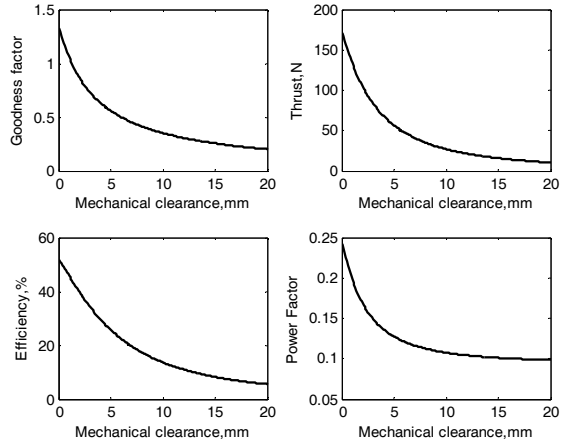

Fig. 5. The motor outputs versus the mechanical clearance

clearance is shown in Fig. 5. It is seen that increasing the mechanical clearance all the output parameters causes to decrease. As a result, in design process, the air-gap should be chosen as short as possible. It should be mentioned that, in some applications such as high-speed traction motors, minimum value of air-gap length is limited. Fig. 6 shows the simulation results of the motor by changing primary width. In this figure, other independent parameters are kept constant. As it is seen in the figure, increasing the primary width, on the one hand, decreases the thrust and the power factor; on the other hand, it increases the efficiency. It is also seen in Fig. 6 that changing the primary width has no effect on goodness factor. Reduction of the thrust by increasing the primary width is because of decreasing the input current under constant voltage due to increasing the motor impedance. According to the obtained results and considering the application of the motor and its limitations, one can develop the design in a way that the motor can produce optimum outputs. Fig. 7 shows the characteristics of the motor outputs versus slip. The variation of the outputs for SLIM in this figure are similar to those in rotating induction machine in which the thrust is comparable with the torque in rotating motor.

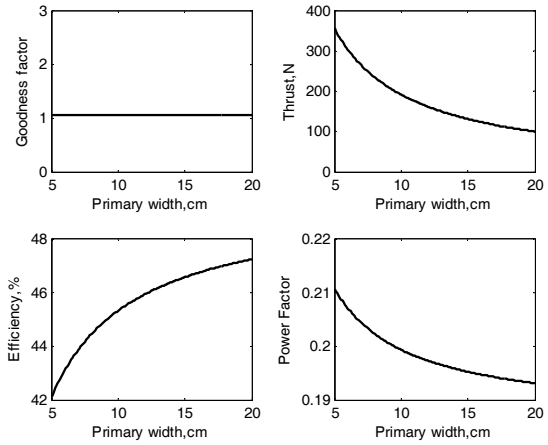

Fig. 6. The motor outputs versus primary width

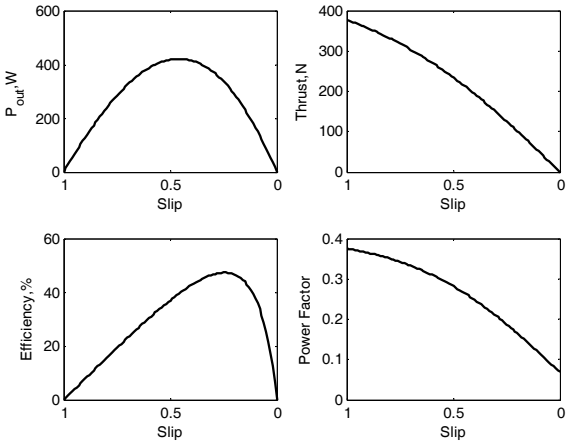

Fig. 7. The motor outputs versus the slip

6. Design Optimization

In an optimization problem, if the independent parameters are defined as $x=(x_1,x_2,...,x_n)$, the object of the design process is to find a vector x such that optimize the predefined function $f(x)$ under some constraints. As seen in the previous section, to design a SLIM, different variables can be chosen for vector x. Considering the results of the investigations performed in section 5, in this paper variables of vector x are chosen as follows: primary current density (J), primary width (W_s), secondary sheet thickness (d), motor slip (s) and the mechanical clearance (g). In addition, the ratio of the primary width to the pole pitch is applied as optimization constraint:

$$0.5 \le \frac{W_s}{\tau} \le 4 \tag{23}$$

Other constraints applied to the design are listed in Table 5.

Table 5. Design variable constraints

Parameter	Minimum value	Maximum value
Primary current density, A/mm2	3	5
Primary width, mm	50	200
Secondary sheet thickness, mm	1	4
Slip	0.1	0.5
Slot width to slot pitch ratio	0.4	0.7
Air gap length, mm	1	15

To optimize the motor, different outputs can be considered as objective function. In this paper, regarding the importance of the efficiency and power factor, the product of them is considered as objective function:

$$f(x)=\eta(x)\times P.F.(x) \tag{24}$$

where x is the optimization variables vector. Other rated specifications of the motor which are not considered as optimization variables, are given in Table 4. In this paper, genetic algorithm is employed for optimization. The genetic algorithm is a method that searches among different variable values and finds a set of parameters to optimize the objective function [18]. The optimal design results obtained by the mentioned method are shown in Table 6. It can be seen that the thrust is close enough to

Table 6. Optimized motor parameter values

Parameter	Optimum value
Primary current density, A/mm2	5
Primary width, mm	191.3
Secondary sheet thickness, mm	1.9
Air gap length, mm	1
Efficiency, %	38.58
Power factor	0.5206
Thrust, N	127.98
Objective function	0.2008

desired value and the objective function is improved from 0.0887 in previous design to 0.2008 in optimal one.

7. Results Validation

In this paper, because of the low speed of the motor, the end effect phenomenon is not considered in the model used for design and optimization. In addition, the permeability of the primary core and the secondary back iron was supposed to be infinity. So, it is necessary to confirm the results of the optimization. To do this, in this section the optimized design is simulated using 2-D finite element method (FEM). Fig. 8 shows the distribution of the flux density in different parts of the SLIM. As it is seen in this figure, the flux density in the air-gap and the secondary sheet is less than 0.4 Tesla in most of the areas. Fig. 9 illustrates the flux paths in the different parts of the motor as it moves in x direction. It can be seen that the flux lines are denser in exit end of the motor. As the motor moves towards right, the flux wave travels left. Induced eddy-current density distribution in the primary and the secondary back iron as well as the secondary sheet is also shown in Fig. 10. It should be mentioned that, the iron loss is considered in efficiency calculation. The efficiency, power factor and thrust are calculated using FEM. The calculation results are compared with FEM results in Table 7. As seen in this table, the thrust obtained by FEM is slightly lower than that of obtained by analytical calculations. It is because of the end effect phenomenon

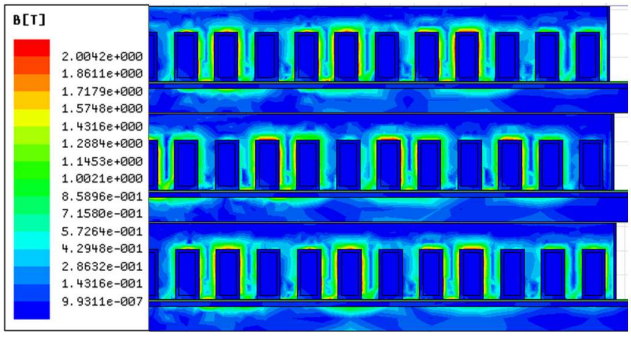

Fig. 8. Flux density distribution in different parts of SLIM

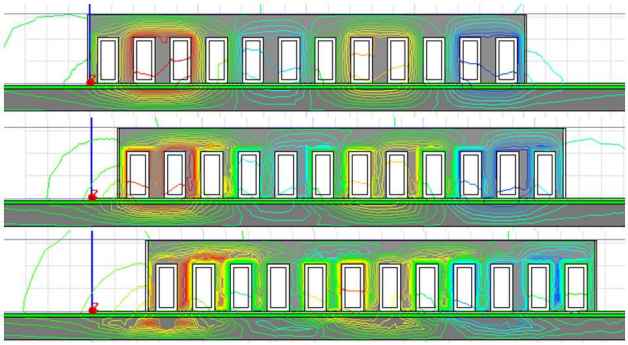

Fig. 9. Flux paths in the SLIM

which is not considered in analytical model. However, the results of the two methods are in good agreement with each other.

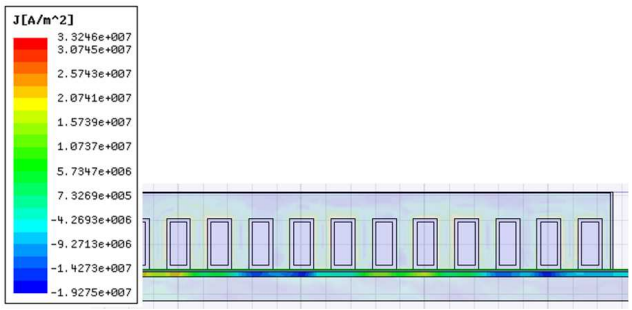

Fig. 10. Eddy-current distribution in the SLIM

Table 7. The calculation and FEM results

Parameter	Analytical model	FEM
Efficiency, %	38.58	35.7
Power factor	0.5206	0.504
Thrust, N	127.98	119.6
Objective function	0.2008	0.1799

8. Conclusion

A simple algorithm is proposed to design the single-sided linear induction motor. The genetic algorithm is employed to maximize the efficiency and the power factor. The results show a noticeable improvement in the objective function. Experimental results are used to confirm the precision of the equivalent circuit model. The effectiveness of the optimization is confirmed by finite element method. The FEM results, in which the end effect is considered, are in good agreement with the analytical results. This confirms the validity of the proposed optimal design in low speeds.

References

[1] S. Nonaka and T. Higuchi, "Elements of linear induction motor design for urban transit", *IEEE Trans. on Magnetics*, Vol. 23, No. 5, pp. 3002-3004, September 1989.

[2] S. Yoon, J. Hur and D. Hyun, "A method of optimal design of single-sided linear induction motor for transit", IEEE Trans. on Magnetics, Vol. 33, No. 5, pp. 4215-4217, September 1997.

[3] W. Xu, J. Zhu, L, Tan, Y. Guo, S, Wang, and Y. Wang, "Optimal design of a linear induction motor applied in transportation", IEEE International Conference on Industrial Technology, pp. 1-6, 2009.

[4] S. A. Nasar and L. del Cid, "Certain approaches to the analysis of single-sided linear induction motors",

Proceedings of IEE, Vol. 120, No. 4, pp. 477-483 April 1973.

[5] G. Dawson, A. R. Eastham, J. F. Gieras, R. Ong and K. Ananthasivam, "Design of linear induction drives by field analysis and finite-element techniques", IEEE Transactions on Industry Applications, Vol. IA-22, No. 5, pp. 865-873, September/October 1986.

[6] R. M. Pai, I. Boldea, and S. A. Nasar, "A complete equivalent circuit of a linear induction motor with sheet secondary", IEEE Trans. on Magnetics, Vol. 24, No. 1, January 1988.

[7] S. Nonaka, "Investigation of equivalent circuit quantities and equations for calculation of characteristics of single-sided linear induction motors (LIM)", Electrical Engineering in Japan, Vol. 117, No. 2, pp. 107-121, 1996.

[8] S. Osawa, M. Wada, M. Karita, D. Ebihara and T. Yokoi, "Light-weight type linear induction motor and its characteristics", IEEE Trans. on Magnetics, Vol. 28, No. 4, September 1992.

[9] M. Kitamura, N. Hino, H. Nihei and M. Ito, "a direct search shape optimization based on complex expressions of 2-dimentional magnetic fields and forces", IEEE Trans. on Magnetics, Vol. 34, No. 5, September 1998.

[10] B. Laporte, N. Takorabet and G. Vinsard, "An approach to optimize winding design in linear induction motors", IEEE Transactions on Magnetics, Vol. 33, No. 2, March 1997.

[11] T. Mishima, M. Hiraoka and T. Nomura, "A study of the optimum stator winding arrangement of LIM in maglev systems", IEEE International Conference on Electric Machines Drives, IEMDC, May 2005.

[12] Hassanpour Isfahani, H. Lesani and B. M. Ebrahimi, "Design Optimization of Linear Induction Motor for Improved Efficiency and Power Factor", IEEE International Conference on Electric Machines Drives, IEMDC, 2007, pp. 988-991.

[13] Hassanpour Isfahani, B. M. Ebrahimi, and H. Lesani, "Design Optimization of a Low-Speed Single-Sided Linear Induction Motor for Improved Efficiency and Power Factor", IEEE Trans. on Magnetics, Vol. 44, No. 2, February 2008.

[14] Lucas, Z. Nasiri G. and F. Tootoonchian, "Application of an imperialist competitive algorithm to design of linear induction motor", Elsevier, Energy Conversion and Management, Vol. 51, pp. 1407-1411, 2010.

[15] J. F. Gieras, Linear induction drives, Oxford University Press, Inc., New York, 1994.

[16] Boldea, S. A. Nasar, linear motion electromagnetic devices, Taylor & Francis, New York 2001.

[17] IEEE Std. 112™-2004 (Revision of IEEE Std 112-1996) "IEEE standard test procedure for polyphase induction motors and generators", November 2004.

[18] S. Sumathi and Surekha P., Computational intelligence paradigms: theory and applications using MATLAB, CRC Press, Taylor & Francis, New York 2010.

Abbas Shiri was born in Hashtrood, Iran in 1980. He received the B.Sc. degree from Tabriz University and M.Sc. degree from Iran University of Science and Technology (IUST) both in electrical engineering in 2004 and 2006, respectively. He is currently working toward Ph.D. degree in electrical engineering at IUST. His areas of research interests include linear electric machines, electromagnetic systems and actuators, electrical machine design and modeling.

Abbas Shoulaie was born in Isfahan, Iran, in 1949. He received the B.Sc. degree from Iran University of Science and Technology (IUST), Tehran, Iran, in 1973, and the M.Sc. and Ph.D. degrees in electrical engineering from U.S.T.L, Montpellier, France, in 1981 and 1984, respectively. He is a Professor at the department of Electrical Engineering, IUST. He is the author of more than 100 journal and conference papers in the field of power electronics, electromagnetic systems, electrical machine, linear machine and HVDC.